Enantioselective DNA Threading Dynamics by Phenazine-Linked $[Ru(phen)_2dppz]^{2+}$ Dimers

Björn Önfelt, Per Lincoln, and Bengt Nordén*

Contribution from the Department of Physical Chemistry, Chalmers University of Technology, S-412 96 Gothenburg, Sweden

Received October 9, 2000

Abstract: The interactions between the stereoisomers of the chiral bis-intercalator $[\mu\text{-C4(cpdppz)}_2\text{-(phen)}_4\text{Ru}_2]^{4+}$ and DNA reveal interesting dynamic discrimination properties. The two enantiomers Δ-Δ and Λ-Λ both form very strong complexes with calf thymus DNA with similar thermodynamic affinities. By contrast, they display considerable variations in their binding kinetics. The Δ-Δ enantiomer has higher affinity for calf thymus DNA than for $[poly(dA\text{-}dT)]_2$, and the association kinetics of the dimer to DNA, as well as to polynucleotides, requires a multiexponential fitting function. The dissociation reaction, on the other hand, could be described by a single exponential for $[poly(dA\text{-}dT)]_2$, whereas two exponentials were required for mixed-sequence DNA. To understand the key mechanistic steps of the reaction, the kinetics was studied at varied salt concentration for different choices of DNA and chirality of the threading complex. The enantiomers were found to have markedly different dissociation rates, the Λ-Λ enantiomer dissociating about an order of magnitude faster than the Δ-Δ enantiomer. Also, the salt dependence of the dissociation rate constants differed between the enantiomers, being stronger for the Λ-Λ enantiomer than for the Δ-Δ enantiomer. Since the dissociation reaction requires unthreading of bulky parts of the bis-intercalator through the DNA helix, a considerable conformational change of the DNA must be involved, possibly defining the rate-limiting step.

Introduction

Many attempts have been made to find compounds that combine strong DNA affinity with slow dissociation from DNA, properties of which especially the latter are considered to be important for antitumor activity.[1] Natural antibiotics that bind to DNA by bis-intercalation,[2−4] have stimulated the approach to achieve high affinity for DNA by linking two or more subunits of known DNA mono-intercalators to form poly-intercalating compounds. In this way novel bis-intercalators,[5−16] but also tris-, tetra-, and even hexamers of intercalating drugs have been synthesized,[17−21] some of which exhibit high affinity and extremely slow dissociation rates. Another property that has been found to give rise to slow interaction kinetics with DNA is the threading of bulky subunits of the ligand through the core of the DNA. An example of a threading compound is the natural product antibiotic nogalamycin, which has to thread a bulky sugar moiety through the stack of DNA bases to reach its final binding mode in which one sugar moiety binds in the minor and the other in the major groove.[22−25] Earlier studies have shown the kinetic interaction of nogalamycin and DNA to be greatly dependent on base sequence; for example, the dissociation was found to be about 150 times faster from $[poly(dA\text{-}dT)]_2$ compared to that from $[poly(dG\text{-}dC)]_2$.[26,27] The metalloglycopeptide, pepleomycin, related to bleomycin, has been proposed to thread its C terminus through the DNA core.[28]

(1) Müller, W.; Crothers, D. M. *J. Mol. Biol.* **1968**, *35*, 251−290.
(2) Leroy, J. L.; Gao, X. L.; Misra, V.; Guéron, M.; Patel, D. J. *Biochemistry* **1992**, *31*, 1407−1415.
(3) Boger, D. L.; Chen, J.-H.; Saionz, K. W. *J. Am. Chem. Soc.* **1996**, *118*, 1629−1644.
(4) Boger, D. L.; Ledeboer, M. W.; Kume, M.; Searcey, M.; Jin, Q. *J. Am. Chem. Soc.* **1999**, *121*, 11375−11383.
(5) Pelaprat, D.; Delbarre, A.; Le Guen, I.; Roques, B. P. *J. Med. Chem.* **1980**, *23*, 1336−1343.
(6) Pothier, J.; Delepierre, M.; Barsi, M.-C.; Garbay-Jaureguiberry, C.; Igolen, J.; Lebret, M.; Roques, B. P. *Biopolymers* **1991**, *31*, 1309−1323.
(7) Robinson, H.; Priebe, W.; Chaires, J. B.; Wang, A. H. J. *Biochemistry* **1997**, *36*, 8663−8670.
(8) Leng, F. F.; Priebe, W.; Chaires, J. B. *Biochemistry* **1998**, *37*, 1743−1753.
(9) Hu, G. G.; Shui, X. Q.; Leng, F. F.; Priebe, W.; Chaires, J. B.; Williams, L. D. *Biochemistry* **1997**, *36*, 5940−5946.
(10) Peek, M. E.; Lipscomb, L. A.; Bertrand, J. A.; Gao, Q.; Roques, B. P.; Garbay-Jaureguiberry, C.; Williams, L. D. *Biochemistry* **1994**, *33*, 3794−3800.
(11) Capelle, N.; Barbet, J.; Dessen, P.; Blanquet, S.; Roques, B. P.; Le Pecq, J.-B. *Biochemistry* **1979**, *18*, 3354−3362.
(12) Gallego, J.; Reid, B. R. *Biochemistry* **1999**, *38*, 15104−15115.
(13) Spielmann, H. P.; Wemmer, D. E.; Jacobsen, J. P. *Biochemistry* **1995**, *34*, 8542−8553.
(14) Larsson, A.; Carlsson, C.; Jonsson, M.; Albinsson, B. *J. Am. Chem. Soc.* **1994**, *116*, 8459−8465.
(15) Rye, H. S.; Yue, S.; Wemmer, D. E.; Quesada, M. A.; Haugland, R. P.; Mathies, R. A.; Glazer, A. N. *Nucleic Acids Res.* **1992**, *20*, 2803−2812.
(16) O'Reilly, F. M.; Kelly, J. M. *J. Phys. Chem. B* **2000**, *104*, 7206−7213.
(17) Laugâa, P.; Markovits, J.; Delbarre, A.; Le Pecq, J.-B.; Roques, B. P. *Biochemistry* **1985**, *24*, 5567−5575.
(18) Atwell, G. J.; Leupin, W.; Twigden, S. J.; Denny, W. A. *J. Am. Chem. Soc.* **1983**, *105*, 2913−2914.
(19) Gaugain, B.; Markovits, J.; Le Pecq, J.-B.; Roques, B. P. *FEBS letters* **1984**, *169*, 123−126.
(20) Wirth, M.; Buchardt, O.; Koch, T.; Nielsen, P. E.; Nordén, B. *J. Am. Chem. Soc.* **1988**, *110*, 932−939.
(21) Lokey, R. S.; Kwok, Y.; Guelev, V.; Pursell, C. J.; Hurley, L. H.; Iverson, B. L. *J. Am. Chem. Soc.* **1997**, *119*, 7202−7210.
(22) Liaw, Y.-C.; Gao, Y.-G.; Robinson, H.; van der Marel, G. A.; van Boom, J. H.; Wang, A. H. J. *Biochemistry* **1989**, *28*, 9913−9918.
(23) Gao, Y.-G.; Liaw, Y.-C.; Robinson, H.; Wang, A. H. J. *Biochemistry* **1990**, *29*, 10307−10316.
(24) Egli, M.; Williams, L. D.; Frederick, C. A.; Rich, A. *Biochemistry* **1991**, *30*, 1364−1372.
(25) Smith, C. K.; Davies, G. J.; Dodson, E. J.; Moore, M. H. *Biochemistry* **1995**, *34*, 415−425.
(26) Fox, K. R.; Waring, M. J. *Biochim. Biophys. Acta* **1984**, *802*, 162−168.
(27) Fox, K. R.; Brassett, C.; Waring, M. J. *Biochim. Biophys. Acta* **1985**, *840*, 383−392

10.1021/ja003624d CCC: $20.00
Published on Web 03/30/2001

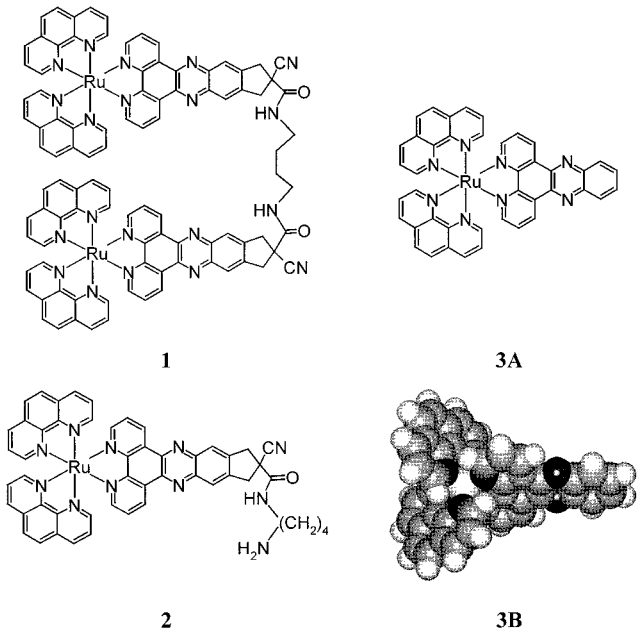

Figure 1. Structures. [μ-C4(cpdppz)$_2$(phen)$_4$Ru$_2$]$^{4+}$ (**1**), [Ru(phen)$_2$-cpdppzC4NH$_2$]$^{2+}$ (**2**), and [Ru(phen)$_2$dppz]$^{2+}$ (**3**). The metal center is chiral, so **1** exists as three stereoisomers, (Δ-Δ, Λ-Λ, and Δ-Λ = *meso*) and **2** and **3** in two enantiomeric forms (Δ and Λ). The absolute configuration Δ is defined in **3B**.

Another compound with an interesting DNA-threading binding mode is NetAmsa, a netropsin−amsacrine hybrid made up of two subunits structurally similar to the minor groove binding antibiotic, netropsin, and the intercalating antileukemia drug, amsacrine.[29] Binding mode, kinetics, and cytotoxicity have been characterized for a few synthetic drugs in the light of a potential DNA-threading mechanism, for example, by varying the position of different subunits on an intercalating moiety to facilitate or obviate threading.[30,31]

We recently reported on the photophysical[32] and DNA binding[33] properties of a novel type of chiral bis-intercalating ruthenium complex, [μ-C4(cpdppz)$_2$(phen)$_4$Ru$_2$]$^{4+}$ (**1** in Figure 1) and its corresponding monomer derivative [Ru(phen)$_2$-cpdppzC4NH$_2$]$^{2+}$(**2**).[34] The monomer [Ru(phen)$_2$dppz]$^{2+}$ (**3**) and structurally similar compounds, such as [Ru(bipy)$_2$dppz]$^{2+}$, have attracted great current interest due to their spectacular photophysical properties upon DNA binding.[35−42] These monomeric compounds are known to intercalate by inserting the dppz ligand between adjacent DNA base pairs and placing the two remaining bidentate ligands in a groove. As to the monomer (**3**) and related compounds, both major groove,[43] and minor groove[44−46] sites have been proposed. While the binding of the monomer (**3**) to DNA is anticipated to be a straightforward intercalation insertion process, bis-intercalation of the dimer (**1**) implies for topological reasons that the binding must involve threading of the bulky Ru(phen)$_2$ moiety either through passage through the DNA or by slinging the bridging chain around two coherently opening base pairs. Flow linear dichroism shows that both dppz moieties of the two Ru centers are intercalated (bis-intercalation), and binding stoichiometry from titration studies as well as molecular modeling indicates that they are separated by two base pairs.[33] This remarkable DNA complex involves a complicated binding process, which is mechanistically interesting as it may throw light on DNA conformational change and base pair opening. Figure 2 defines, schematically, the main possible intermediate bound forms (A−C) on the path towards the thermodynamically most favored binding mode (D). Using optical spectroscopic techniques we have followed the kinetics and conformation of these threading intercalators upon interaction with DNA and, for comparison, also the corresponding monomers, with respect to dependence on ionic-strength, choice of DNA and chirality of the Ru centers. The system is particular in that the size of the Ru(phen)$_2$ moiety is bulkier than that of the subunits of other known threading substances. This is also to our best knowledge the first case of a threading bis-intercalator for which DNA interaction properties have been characterized for opposite enantiomeric forms.

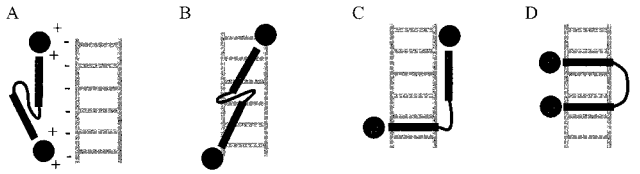

Figure 2. Schematic DNA-interaction modes of the dimer (**1**)**.** (A) *Electrostatic external binding.* (B) *Groove binding.* The subunits positioned in either minor or major groove of DNA. (C) *Mono-intercalation.* One subunit intercalated the other one either in a groove or freely dangling (D) *Bis-intercalation.* Both subunits intercalated, either in the minor or the major groove, the bridging chain residing in the opposite groove.

Materials and Methods

Equilibrium Constants. The extraordinary high DNA affinity for these compounds makes it impossible to measure the equilibrium constant with conventional methods such as absorption titration. We have developed a new technique where the huge increase of the excited-state lifetime and emission quantum yield of the [Ru(phen)$_2$dppz]$^{2+}$ chromophore upon binding to DNA[36] is used to monitor the amount of bound compound in order to determine the binding constant. A mixture

(28) Caceres-Cortes, J.; Sugiyama, H.; Ikudome, K.; Saito, I.; Wang, A. H. J. *Biochemistry* **1997**, *36*, 9995−10005.
(29) Bourdouxhe-Housiaux, C.; Colson, P.; Houssier, C.; Waring, M. J.; Bailly, C. *Biochemistry* **1996**, *35*, 4251−4264.
(30) Tanious, F. A.; Jenkins, T. C.; Neidle, S.; Wilson, W. D. *Biochemistry* **1992**, *31*, 11632−11640.
(31) Searcey, M.; Martin, P. N.; Howarth, N. M.; Madden, B.; Wakelin, L. P. G. *Bioorg. Med. Chem. Lett.* **1996**, *6*, 1831−1836.
(32) Önfelt, B.; Lincoln, P.; Nordén, B.; Baskin, J. S.; Zewail, A. H. *Proc. Natl. Acad. Sci USA* **2000**, *97*, 5708−5713.
(33) Önfelt, B.; Lincoln, P.; Nordén, B. *J. Am. Chem. Soc.* **1999**, *121*, 10846−10847.
(34) C4(cpdppz)$_2$ = *N*,*N*′ bis(cpdppz)-1,4-diaminobutane, cpdppzC4N = *N*-cpdppz-1,4-diaminobutane, cpdppz = 12-cyano-12,13-dihydro-11*H*-8-cyclopenta[*b*]dipyrido[3,2-*h*:2′3′-*j*] phenazine-12-carbonyl, dppz = dipyrido[3,2-*a*:2′,3′-*c*]phenazine, phen = 1,10-phenanthroline.
(35) Olson, E. J. C.; Hu, D.; Hörmann, A.; Jonkman, A. M.; Arkin, M. R.; Stemp, E. D. A.; Barton, J. K.; Barbara, P. F. *J. Am. Chem. Soc.* **1997**, *119*, 11458−11467.
(36) Friedman, A. E.; Chambron, J.-C.; Sauvage, J.-P.; Turro, N. J.; Barton, J. K. *J. Am. Chem. Soc.* **1990**, *112*, 4960−4962.
(37) Hiort, C.; Lincoln, P.; Nordén, B. *J. Am. Chem. Soc.* **1993**, *115*, 3448−3454.
(38) Haq, I.; Lincoln, P.; Suh, D.; Nordén, B.; Chowdhry, B. Z.; Chaires, J. B. *J. Am. Chem. Soc.* **1995**, *117*, 4788−4796.
(39) Lincoln, P.; Broo, A.; Nordén, B. *J. Am. Chem. Soc.* **1996**, *118*, 2644−2653.
(40) Lincoln, P.; Tuite, E.; Nordén, B. *J. Am. Chem. Soc.* **1997**, *119*, 1454−1455.
(41) Erkkila, K. E.; Odom, D. T.; Barton, J. K. *Chem. Rev.* **1999**, *99*, 2777−2795.
(42) Liu, J.-G.; Ye, B.-H.; Zhang, Q.-L.; Zou, X.-H.; Zhen, Q.-X.; Tian, X.; Ji, L.-N. *J. Biol. Inorg. Chem.* **2000**, *5*, 119−128.
(43) Dupureur, C. M.; Barton, J. K. *J. Am. Chem. Soc.* **1994**, *116*, 10286−10287.
(44) Choi, S.-D.; Kim, M.-S.; Kim, S. K.; Lincoln, P.; Tuite, E.; Nordén, B. *Biochemistry* **1997**, *36*, 214−223.
(45) Tuite, E.; Lincoln, P.; Nordén, B. *J. Am. Chem. Soc.* **1997**, *119*, 239−240.
(46) Greguric, I.; Aldrich-Wright, J. R.; Collins, J. G. *J. Am. Chem. Soc.* **1997**, *119*, 3621−3622.

of DNA and complex is gradually diluted and the emission intensity of the sample recorded. Lowering the total concentration drives the equilibrium toward more free dye, seen as a stronger decrease of the emission intensity than expected from dilution solely. Equilibrium constants were obtained by fitting the emission titration data with a McGhee−von Hippel type of noncooperative binding isotherm,[47] with the size of the binding site assumed to be four base pairs. The equilibrium constant was determined at several different salt concentrations ranging from 0.1 to 0.3 M NaCl. Due to the very high affinity of **1** it was impossible to get reliable equilibrium data at lower salt concentrations. The ratio P/Ru[48] was equal to 8, which corresponds to occupation of every second binding site at quantitative binding. All solutions of DNA and dimer were incubated for at least 12 h at room temperature before measurement. Absorption spectra of free **1** in buffer was found to be invariant of concentration in the range 0.1−10 μM, indicating that no significant self-association occurs.

Kinetics. Stopped-flow experiments were made on a computer-controlled instrument from Bio Logic, set up for fluorescence detection. Light from a Hg(Xe) lamp was sent through a monochromator set at 436 nm. The emission channel had a red filter (<540 nm cutoff) preceding the photomultiplier. Typically, five traces were averaged for each output file. Syringes and cuvette were thermostated at 20 ± 1.5 °C by a water jacket. Solutions of calf thymus DNA (ct-DNA) used in stopped-flow measurements were in some of the experiments sonicated on a Sonics and Materials Vibra Cell during 15 min before usage to decrease orientation effects. However, no difference between sonicated and unsonicated samples could be detected. Longer time scale kinetic experiments were carried out on a SPEX fluorolog steady-state fluorometer (temperature set to 20 ± 1 °C). The dissociation reaction was initiated by addition of sodium dodecyl sulfate (SDS) dissolved in buffer (0.012 or 0.03 g SDS/ml buffer, buffer specifications stated below) to an equilibrium mixture of Ru complex and DNA. The volume proportion of SDS solution to equilibrium mixture was 1:4 when the reaction was studied with manual mixing methods and 1:1 when stopped-flow technique was used. The final concentration of SDS was at least 0.6% w/w. The rate of dissociation was confirmed to be independent of the concentration of SDS in the range 0.6−2% w/w.

All kinetic traces $S(t)$ were analyzed by fitting to a sum of exponential terms of amplitude A_i and rate constant k_i, $S(t)=\sum A_i \exp(-k_i t)$, with minimum number of terms to leave no systematic errors in the residuals.

Preparation of Reaction Solutions. All reactions were carried out in aqueous buffers (Tris (5 mM) cacodylate (1 mM), 10 mM in NaCl, pH = 7.22 or phosphate (5 mM), pH = 6.85). Higher salt concentrations were prepared by addition of an aqueous solution of NaCl (4 or 2 M). The concentrations of reactants were determined by absorbance measurements on a UV/vis spectrophotometer (Varian Cary 2300 or Varian Cary 4B). The extinction coefficients used were: $\epsilon_{440\ nm}$ = 20 000 M^{-1} cm^{-1}(Ru)$^{-1}$ for **1**−**3**, $\epsilon_{260\ nm}$ = 6600 M^{-1} cm^{-1} for ct-DNA, $\epsilon_{255\ nm}$ = 8400 M^{-1} cm^{-1} for [poly(dG-dC)]$_2$, and $\epsilon_{262\ nm}$ = 6600 M^{-1} cm^{-1} for [poly(dA-dT)]$_2$.

Flow Linear Dicroism. Linear Dichroism (LD) is defined as the difference in absorbance of light linearly polarized parallel and perpendicular to a macroscopic axis of orientation (the flow direction):

$$\mathrm{LD}(\lambda) = A_{\mathrm{II}}(\lambda) - A_z(\lambda) \qquad (1)$$

Samples of ruthenium complex and [poly(dA-dT)]$_2$ were oriented in flow gradient (900 rpm) in a Couette flow cell with an outer rotating cylinder and LD spectra measured on a Jasco J-500 spectrodichrometer.[49−51]

Chemicals. [μ-C4(cpdppz)$_2$-(phen)$_4$Ru$_2$]$^{4+}$ (**1**), [Ru(phen)$_2$cpdppz-C4NH$_2$]$^{2+}$ (**2**), and [Ru(phen)$_2$dppz]$^{2+}$ (**3**) were synthesized as described elsewhere.[33,37] Calf thymus DNA (Sigma) was dissolved in buffer and filtered through a 0.8 μm Millipore filter before use. The lyophilized sodium salts of [poly(dG-dC)]$_2$ and [poly(dA-dT)]$_2$ (Pharmacia Biotech) were used as obtained.

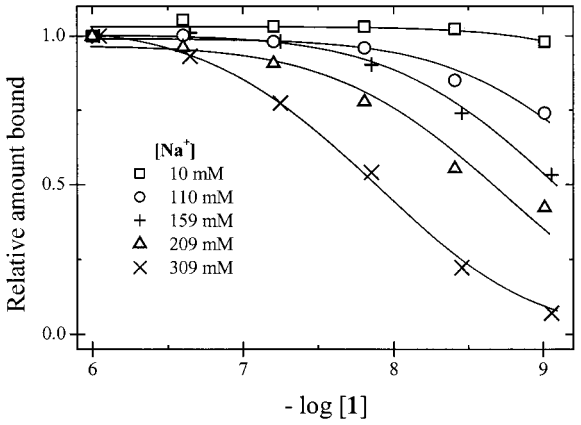

Figure 3. Dilution titrations for Δ-Δ **1** bound to ct-DNA. The graph shows the normalized emission intensity compensated for dilution, reflecting the relative amount of bound complex as a function of log concentration of compound. Solid lines represent best fits with McGhee−von Hippel noncooperative binding isotherms. Dilutions series were performed at the salt concentrations indicated in the graph.

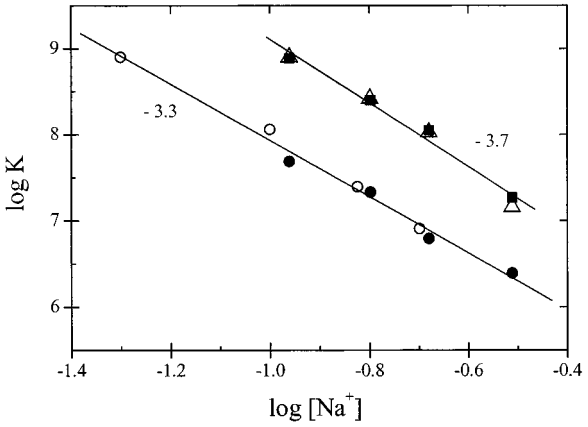

Figure 4. Salt dependence of the thermodynamic equilibrium constant for the binding of the two enantiomers of **1** to ct-DNA (top line, Δ = Δ-Δ and ■ = Λ-Λ) and to [poly(dA-dT)]$_2$ (bottom line, ● = Δ-Δ).The bottom line also shows the excellent agreement between the thermodynamic and kinetically determined equilibrium constant for [poly(dA-dT)]$_2$ (○ = Δ-Δ, see text). Slopes as indicated.

Results

Equilibrium Binding. Figure 3 shows an example of a set of equilibrium dilution titrations at different salt concentrations of Δ-Δ **1** in the presence of ct-DNA. The graph shows the normalized emission intensity compensated for dilution, reflecting the relative amount of bound complex as a function of concentration of compound on a logarithmic scale. Equilibrium constants were obtained by fitting the titration data with a McGhee−von Hippel type of noncooperative binding isotherm,[47] shown in Figure 4 for binding of the two enantiomers of **1** to ct-DNA and the Δ-Δ enantiomer to [poly(dA-dT)]$_2$ at different salt concentrations. The two enantiomers bind to ct-DNA with very similar values of the equilibrium constant at all studied salt concentrations. The slope of the log K vs log [Na^+] plot agrees well with the value predicted by polyelectrolyte theory for an intercalating molecule carrying 4 positive charges: experimental slope of ∼−3.7 for both enantiomers, to be

(47) Lincoln, P. *Chem. Phys. Lett.* **1998**, *288*, 647−656.

(48) The DNA-to-ligand ratio in the experiments is given by the ratio P/Ru, where P is the concentration of DNA phosphate (=[DNA bases]) and Ru the concentration of Ru(phen)$_2$dppz subunits. Note that for a nearest neighbor-exclusion model, saturation of the DNA occurs at P/Ru = 4 for all three compounds **1**−**3**.

(49) Nordén, B. *Appl. Spectrosc. Rev.* **1978**, *14*, 157−248.

(50) Nordén, B.; Tjerneld, F. *Biopolymers* **1982**, *21*, 1713−1734.

(51) Nordén, B.; Kubista, M.; Kurucsev, T. *Q. Rev. Biophys.* **1992**, *25*, 51−170.

Table 1. Equilibrium Constants (K/M^{-1}) at 20 °C

	ct-DNA		[poly(dA-dT)]$_2$
[Na$^+$]/mM	Λ-Λ	Δ-Δ	Δ-Δ
110	$7.7 \pm 3 \times 10^8$	$8.0 \pm 2.4 \times 10^8$	$4.8 \pm 4 \times 10^7$
159	$2.5 \pm 0.7 \times 10^8$	$2.6 \pm 0.5 \times 10^8$	$2.1 \pm 1.5 \times 10^7$
209	$1.1 \pm 0.4 \times 10^8$	$1.1 \pm 0.5 \times 10^8$	$6.2 \pm 2.5 \times 10^6$
309	$1.8 \pm 0.5 \times 10^7$	$1.4 \pm 0.4 \times 10^7$	$2.5 \pm 1 \times 10^6$

compared with the predicted value −3.76. The apparent linearity of the log K vs log[Na$^+$] plot could justify extrapolation of the binding constants to 50 mM salt concentration, where the equilibrium constants for the enantiomers of the monomeric compound **3** have been determined.[38] At 50 mM [Na$^+$] (20 °C) K was estimated to $\sim 1.7 \times 10^{10}$ M^{-1} for the enantiomers of **1**. This value can be compared with the binding constants for the enantiomers of **3** (25 °C, 50 mM NaCl), reported to 3.2×10^6 for the Δ enantiomer and 1.7×10^6 for the Λ enantiomer. The slope log K vs log[Na$^+$] reported for the monomers are about half (−1.9 for Δ and −2.1 for Λ) of that found here for the dimers.[38] Since this leads to a quite different ionic-strength dependence, the comparison with the extrapolated values of the equilibrium constants should be taken with some caution. However, the dimer binding constants are consistent with earlier reports that dimeric DNA-intercalators have a magnitude of free energy of binding that is less than twice that of the corresponding monomers.[8,17] The affinity of Δ-Δ **1** to [poly(dA-dT)]$_2$ was found to be smaller than for ct-DNA (Table 1). Also the ionic-strength dependence for the interaction, with a slope of −3.3 (Figure 4) appears to be somewhat smaller than with ct-DNA. Preliminary results indicate that the affinity of Δ-Δ **1** to [poly(dG-dC)]$_2$ is similarly smaller compared to ct-DNA (data not shown), which indicates more specific interactions with the latter than a simple A-T or G-C preference.

Kinetics. The dissociation kinetics of the three stereoisomers of **1** from ct-DNA has been investigated at various salt concentrations (see Figure 5A and Table 2). A double exponential fitting function was generally required to fit these reaction rate traces. Interestingly, there is a distinct difference between the dissociation rates as a function of salt, for the two enantiomers, despite their very similar binding equilibrium constants. The ionic strength dependence of dissociation of **1** from ct-DNA is clearly stronger for the Λ-Λ compared to the Δ-Δ enantiomer. Reaction rates described by double exponentials may be represented by an effective lifetime according to $\tau_{\text{eff}} = 1/(k_1A_1 + k_2A_2)$.[52] Using this approach a similar difference is noted, although with slightly stronger salt dependencies as the preexponential factors change with ionic strength (Supporting Information). In contrast to the case of ct-DNA, the dissociation of Δ-Δ **1** from [poly(dA-dT)]$_2$ can be fitted with a single exponential, and a linear dependence with a slope of −2.4 is seen in Figure 5B. Dissociation of Δ-Δ **1** from [poly(dG-dC)]$_2$ is dominated by a slow phase (amplitude >91%) and the associated rate constants (at [Na$^+$] = 25 − 100 mM) show an ionic-strength dependence similar to that found with [poly(dA-dT)]$_2$ (Supporting Information). For comparison we studied also the ionic-strength dependence of the dissociation of the monomers Δ-**2** and Δ-**3** from [poly(dA-dT)]$_2$ (Figure 5B). Also here one exponential was sufficient to fit the experimental curves. As expected, the non-threading monomer **3** dissociates with a very much higher rate than the threading mono-intercalator **2** and, in particular, the bis-intercalator **1**. However, despite the large difference in dissociation rate between **2** and **3**, the ionic-strength dependencies of their dissociation rates were similar, the corresponding slopes in the log k vs log[Na$^+$] plot being −0.12 for **2** and −0.09 for **3**. These ionic-strength dependencies are remarkably small compared to what has been found for other intercalators carrying two positive charges; for example, propidium gives a slope of −0.85 in a similar graph.[53] However, a lower ionic-strength dependence (slope = −0.3) has been reported for the dicationic threading intercalators, which bind with a charged side chain in each groove of the DNA.[30,52]

Figure 6 shows the association rate of Δ-Δ **1** binding to [poly(dA-dT)]$_2$ as a function of ionic strength, studied with stopped-

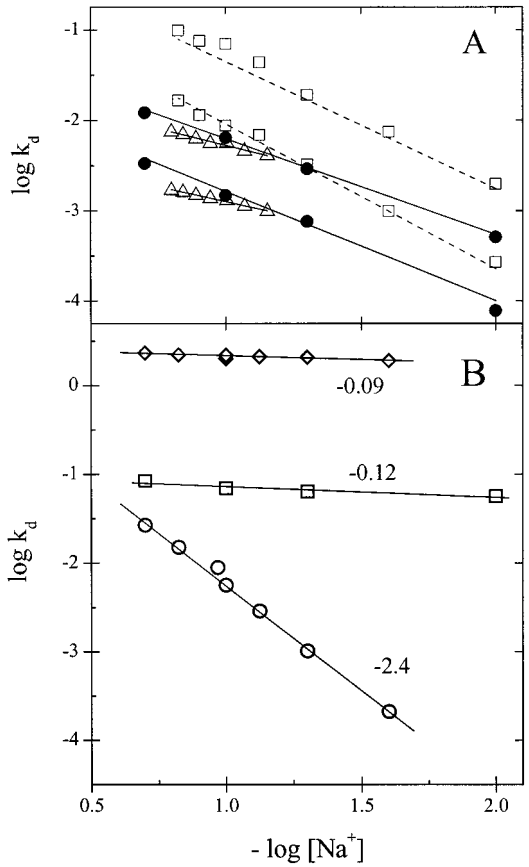

Figure 5. (A) Rates of dissociation of **1** from ct-DNA as a function of salt concentration. The dissociation traces are fitted by a two-exponential function ($A_1\ e^{-k_{d1}t} + A_2\ e^{-k_{d2}t}$) in order to get a good fit: the plotted k_d values correspond to the two exponentials (● = Δ-Λ (*meso*), Δ = Δ-Δ, and □ = Λ-Λ). The lines represent the case when the data have been fitted with the restriction that the logaritmic value of the calculated rate constants should be linearly dependent on log [Na$^+$] (slopes are shown in Table 2). P/Ru = 40 for Λ-Λ and Δ-Λ and 47 for Δ-Δ. (B) Salt dependence of the dissociation rate of Δ [Ru(phen)$_2$dppz]$^{2+}$-systems with [poly(dA-dT)]$_2$ (○ = **1**, □ = **2**, and ◇ = **3**). Slopes as indicated. The binding density (P/Ru) was 40 in all cases.

Table 2. Salt Dependence of the Dissociation of the Diastereomers of **1** from DNA

	slope[a]		
compound	k_{d1}[b]	k_{d2}[c]	k_{eff}[d]
Δ-Δ	−0.74	−0.66	−1.0
Δ-Λ	−1.1	−1.2	−1.4
Λ-Λ	−1.4	−1.6	−1.7

[a] Slope = $-\delta$ log k_d/δ log[Na$^+$] (see Figure 5). [b] Largest rate constant in the biexponential fit. [c] Smallest rate constant in the biexponential fit. [d] Calculated from experimental data according to $k_{\text{eff}} = k_1A_1 + k_2A_2$ (where A is the normalized preexponential factor). Error levels estimated at ±10%.

(52) Tanious, F. A.; Yen, S.-F.; Wilson, W. D. *Biochemistry* **1991**, *30*, 1813−1819.

(53) Wilson, W. D.; Krishnamoorthy, C. R.; Wang, Y.-H.; Smith, J. C. *Biopolymers* **1985**, *24*, 1941−1961.

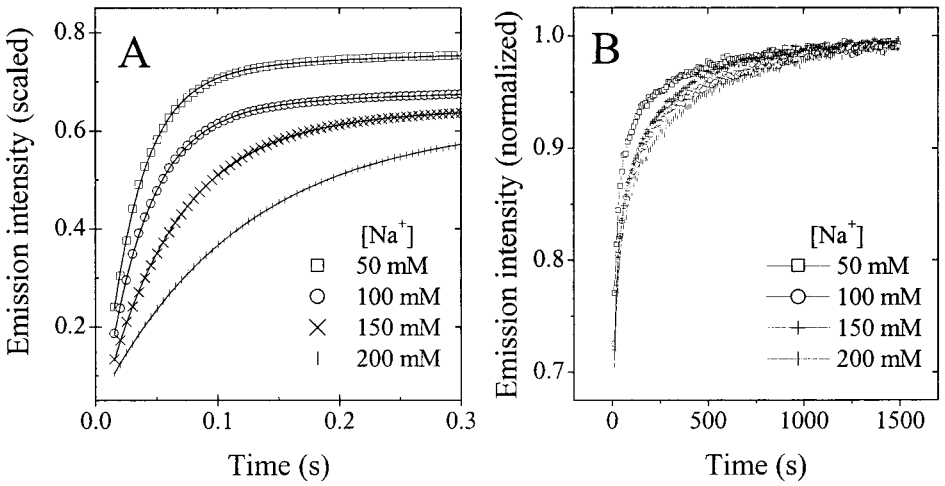

Figure 6. Association of Δ-Δ **1** to [poly(dA-dT)]$_2$ as measured from change in emission, in A with stopped-flow (emission collected above 540 nm, excitation at 436 nm) and in B with manual mixing (emission at 625 nm, excitation at 440 nm). Traces in B have been normalized at 1500 s and the traces in A scaled to overlap with the traces in B at $t = 11$ s. The solid curves shown in A are double exponential fits to the reaction traces up to $t = 0.7$ s.

Table 3. Kinetic Constants for the Interaction of Δ-Δ **1** with [poly(dA-dT)]$_2$

[Na$^+$]/ mM	k_{a1}/s^{-1}	A_{a1}[a] (%)	k_{a2}/s^{-1}	A_{a2}[a] (%)	$k_d \times 10^3$/ s^{-1}	$K_{kinetic}$[b]/ M^{-1}
50	37	69	7.2	7	1.0	8.2×10^8
100	29	63	4.4	6	5.6	1.1×10^8
150	17	62	1.6	6	15	2.5×10^7
200	9.7	50	4.1	14	27	7.9×10^6

[a] Approximate percentage of total emission increase upon binding associated with indexed rate constant. [b] Calculated according to eq 2, using k_{a1}, k_d and [DNA] = 45.23 μM, P/Ru = 40. Error levels estimated at ±15% for the amplitudes and ±15% for the rate constants.

flow as well as manual mixing technique. The association reaction is complex, with three to four exponentials required to fit the experimental data for the first 30 s of the reaction (results not shown). Despite the complexity of the association of Δ-Δ **1** to [poly(dA-dT)]$_2$ we found that the quotient of the initial bimolecular association and the dissociation rate constants gave a kinetically determined equilibrium constant in close agreement with the thermodynamic equilibrium constant obtained from steady-state measurements. Fitting the first 0.7 s of the reaction (Figure 6A) with a double exponential function, gives two apparent association rate constants (k_{a1} and k_{a2} in Table 3). Assuming a consecutive mechanism (see below), dividing the largest of those rate constants (k_{a1}) by the concentration of binding sites ([DNA]) and the dissociation rate constant found at the same ionic strength (k_d in Table 3) yields the kinetic equilibrium constant (eq 2).

$$K_{kinetic} = \frac{k_{a1}}{k_d[\mathrm{DNA}]} \qquad (2)$$

Figure 4 compares equilibrium constants determined with kinetic and thermodynamic methods (for the kinetic constants see Table 3). The good agreement between the two approaches is interesting as it implies certain conditions on the mechanistic model (see Discussion).

Figure 7 compares the rates of association of Δ-Δ **1** to [poly(dA-dT)]$_2$ and [poly(dG-dC)]$_2$. Obviously, the emission intensity, which increases upon binding, reaches a significant level much faster in [poly(dA-dT)]$_2$. This could be due either to faster intercalation with [poly(dA-dT)]$_2$ or to a high emission quantum yield for precursory, nonintercalating intermediates formed with

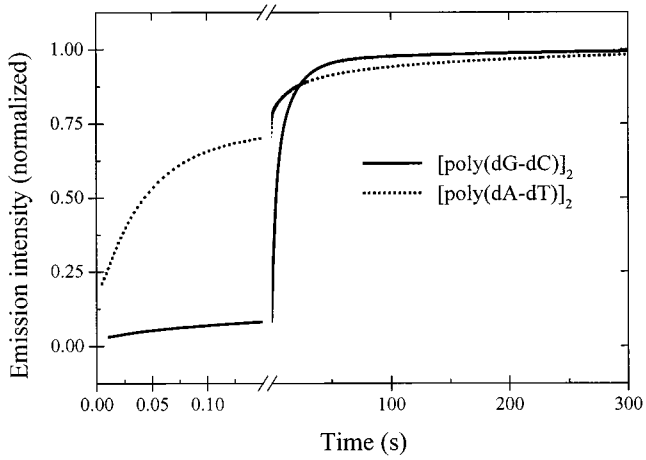

Figure 7. Stopped-flow kinetics association of Δ-Δ **1** to [poly(dA-dT)]$_2$ and [poly(dG-dC)]$_2$. The time scale has been divided into two parts, one showing the fast association and one showing the reaction up to 300 s. The concentration of nucleotide (phosphates) was 367 μM for [poly(dA-dT)]$_2$ and 400 μM for [poly(dG-dC)]$_2$, the ratio (P/Ru) was 40 in both cases, and [NaCl] = 200 mM. The traces are normalized to the end-value given by their respective multiexponential fits of the first 500 s of the reaction.

[poly(dA-dT)]$_2$ compared to [poly(dG-dC)]$_2$. However, the observation that the semi-rigid groove binding dimer [Ru(phen)$_2$-{dppz(11-11′)dppz}Ru(phen)$_2$]$^{4+}$ is nonemissive upon binding to DNA, although it luminesces in organic solvents,[54] indicates that intercalation is indeed a prerequisite for significant quantum yield. We therefore conclude faster intercalation of Δ-Δ **1** to [poly(dA-dT)]$_2$ than to [poly(dG-dC)]$_2$. However, although the first phase of the association to [poly(dA-dT)]$_2$ is fast, there is also a very slow phase of the reaction with an associated rate constant of approximately 10^{-3} s^{-1}. This slow phase, furthermore, corresponds to a relatively large increase in LD signal. When following the shape of the LD spectrum as a function of time, it is evident that it does not change significantly on the long time scale. Principal component analysis clearly shows that all spectra are well described by a single component (Supporting Information). This observation, together with the overall increase in LD signal, makes us conclude that there is no significant change in binding geometry but that it is the orientation of the

(54) Lincoln, P.; Nordén, B. *Chem. Commun.* **1996**, 2145−2146.

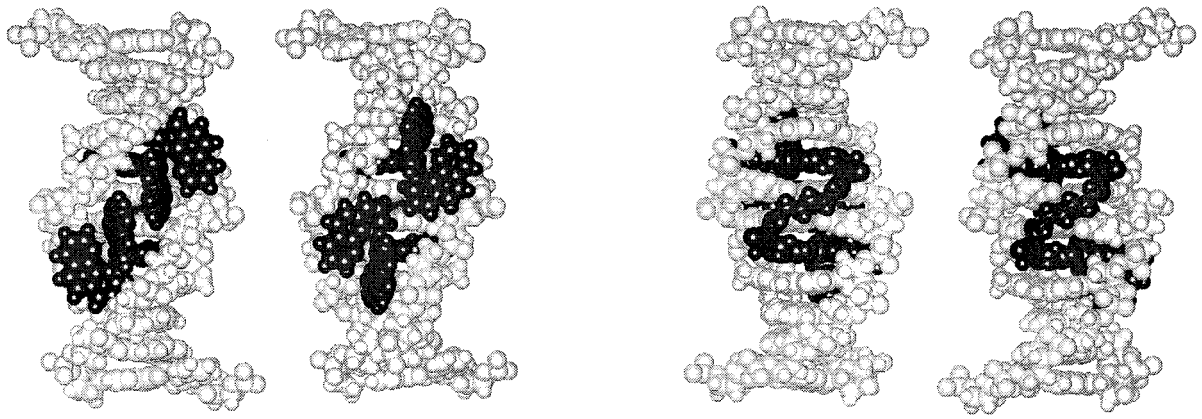

Figure 8. Molecular models of the binding geometry of **1** to DNA. The left pair of structures shows the minor groove, with the Δ-Δ enantiomer to the left and the Λ-Λ enantiomer to the right. The right pair of structures shows the major groove where the linker is situated, Δ-Δ enantiomer to the right and Λ-Λ enantiomer to the left. The structures of Δ-Δ and Λ-Λ forms of **1** bound to a duplex decanucleotide were constructed by energy minimization with the Amber force-field in the HyperChem software package.

DNA that increases. This is, however, not mainly a global orientation increase of the DNA, since the increase in LD of the metal complex absorption is not matched by the LD of the absorption band of the DNA bases (258 nm) (not shown). Instead, the orientation increase appears to be a result of a local stiffening of the DNA in the neighborhood of bound complexes, possibly caused by a redistribution of the initially bound bis-intercalated complexes.

Discussion

A first important observation in this study is the strong binding that the dimer (**1**) displays upon interaction with DNA, and which involves a threading topology since LD shows the binding to be bis-intercalative.[33] Despite the potentially discriminatory orientations of the two auxiliary phenantroline ligands (see below), rather small variations are observed between the binding affinities of opposite enantiomers, Δ-Δ and Λ-Λ, as well as between their ionic-strength dependencies (Table 1, Figure 4). This fact could seem to be in conflict with the remarkably different luminescence properties of the DNA-bound enantiomers.[37,55] However, this luminescence difference appears to be the result of only a very minor structural difference, the dppz moiety penetrating slightly deeper into the base stack for the Δ enantiomers, rather than one of major importance for the stability (see below).[37]

By contrast, the kinetic parameters vary markedly between opposite enantiomers, indicating that they differ considerably with respect to activation barriers to threading. Before we shall discuss the mechanistic origin of this difference, let us consider the salt dependence of the binding (equilibrium) constant and of the binding and dissociation kinetics.

Equilibrium Binding. The simple polyelectrolyte model of Manning[56] has been applied by others [53,57−59] to yield the salt dependence of the equilibrium constant K for the binding of charged ligands to DNA. For a bis-intercalator carrying four positive charges, the slope in a log K vs log[Na^+] diagram is predicted to be −3.76, in excellent agreement with the experimental slope for the enantiomers of **1** with DNA being approximately −3.7 for both Δ-Δ and Λ-Λ (Figure 4). For the binding of Δ-Δ **1** to [poly(dA-dT)]$_2$, the salt dependence was somewhat smaller (slope = −3.3).

Depending on the chirality of the Ru center (Δ or Λ), the two phenanthroline ligands that are not intercalated will position themselves differently with respect to the walls of the DNA groove in which the complex is sitting. Figure 8 depicts the binding geometry of **1** concluded from LD data, with the Ru atoms located in the minor groove.[44−46] The two phenanthroline ligands will be pointing along the direction of the groove for the Δ-Δ enantiomer while they will be perpendicular to the groove for the Λ-Λ complex. A similar set of diastereomeric arrangements would apply also if the ruthenium atoms are sitting in the major groove.[43] These mainly steric differences in binding geometry could be expected to give rise to differences in the equilibrium constant. The more snug fit in the case of the Δ-Δ complex, with the two phen ligands located along the groove, allows the dppz ligand to be more deeply inserted into its intercalation pocket. Since the MLCT excited state of Ru(phen)$_2$dppz is rapidly quenched by water,[32,35] this observation is consistent with the higher fluorescence quantum yield invariably found for the Δ-enantiomers of dppz−Ru complexes bound to nucleic acids. Although monomeric Ru complexes attain a rather low level of enantioselectivity of binding, it is still somewhat surprising that the binding constants are similar for Δ-Δ **1** and Λ-Λ **1**. This make us conclude that the position of the phen ligands do not make any significant steric (repulsive) free energy difference and that the attractive forces, electrostatic interaction (charge 4+) and hydrophobic effects, are the main determinants for the free energy of binding.

Kinetics. All stereoisomers of **1** dissociate very slowly from ct-DNA, [poly(dA-dT)]$_2$ as well as from [poly(dG-dC)]$_2$ (Figure 5 and Supporting Information). This must be because the dissociation reaction involves threading of the bulky parts of the compounds between the strands of the DNA (passing from D, C to A, B in Figure 2). Unthreading involves a substantial conformational change of the DNA helix, probably both opening and unstacking of base pairs. Interestingly, the three stereoisomers have all different dissociation rates from ct-DNA (Figure 5A) and [poly(dA-dT)]$_2$,[33] indicating that the chirality of the Ru center is important for the threading mechanism. At all studied salt concentrations Λ-Λ **1**, in which the Ru ligands form a left-handed propeller, dissociates faster than the *meso* (Δ-Λ) diastereomer, which in turns dissociates faster than Δ-Δ **1** (right-handed propeller, Figure 1). The rates found for the *meso* diastereomer are more like that of the Δ-Δ form, possibly reflecting that the dissociation of the Δ subunit of the *meso* diastereomer acts as an anchor slowing down the dissociation.

(55) Lincoln, P.; Önfelt, B.; Nordén, B. Manuscript in preparation.
(56) Manning, G. S. *J. Chem. Phys.* **1969**, *51*, 924−933.
(57) Anderson, C. F.; Record, M. T. *Annu. Rev. Phys. Chem.* **1995**, *46*, 657−700.
(58) Wilson, W. D.; Lopp, I. G. *Biopolymers* **1979**, *18*, 3025−3041.
(59) Hopkins, H. P.; Wilson, W. D. *Biopolymers* **1987**, *26*, 1347−1355.

Another important observation is that the salt dependency of the dissociation rates differ significantly between the three stereoisomers (Table 2, Figure 5A). The rate constant for Λ-Λ **1** has a stronger dependence on the salt concentration than that of Δ-Δ **1**. This difference is interesting since the salt dependence of the dissociation constant, most likely, is directly dependent on the properties of the rate-limiting step (see below).

The dissociation of an equilibrated sample of Δ-Δ **1** and $[poly(dA\text{-}dT)]_2$ can be described by a single exponential, for both the emission and LD kinetic traces, indicating effectively only a single bound species with one rate-limiting step in the dissociation mechanism. Also dissociation of Δ-Δ **1** from $[poly(dG\text{-}dC)]_2$ is dominated by a single phase (Supporting Information). We believe that the double exponential found for ct-DNA originates from minor variations due to the sequence heterogeneity of different binding geometries along the DNA rather than the coexistence of geometrically different bound forms. Assuming that the dissociation from ct-DNA follows the same mechanism as from $[poly(dA\text{-}dT)]_2$ it is thus unlikely that the double exponential arises from sequential steps.

Wilson and co-workers have presented a model for the binding of a charged intercalator to DNA[53] consisting of two steps, the first being the formation of a loosely bound complex between the drug and the DNA. Electrostatic attraction is assumed to be the only interaction in this first intermediate. The subsequent step(s) is intercalation of the drug, possibly rate-limited by some conformational change of the DNA (opening of an intercalation pocket). According to their approach the slope in the log k_d vs log[Na^+] plot is predicted to be 1.08 for **1**, which is approximately in the middle of the wide interval of slopes that we have observed for the present cases of chirality and nucleotides (Table 2). However, due to the large variation of slopes obtained we conclude that this simple electrostatic model is unable to account for the salt dependency of the dissociation rate.

As to what properties give rise to the different salt dependencies for the stereoisomers, we propose that the faster dissociation and the stronger ionic-strength dependence of the dissociation rate constant observed for the Λ-Λ enantiomer is due to a smaller conformational change of the DNA associated with the unthreading of this enantiomer compared to the Δ-Δ enantiomer. In bound form the positively charged ruthenium complex is likely to interact with the negative phosphate charges of both strands, thus acting to stabilize the double helix. Somewhere along the dissociation pathway this electrostatic interaction between ruthenium and the phosphates is compensated by a Na^+−phosphate interaction. The significance of this compensation upon the rate-limiting step is reflected in the ionic strength dependence for the dissociation constant.

Not only the electrostatic (enthalpic) interaction of the ruthenium compound with polyelectrolyte DNA, but also the dynamic (entropic) behavior of DNA and the DNA complex as a function of salt concentration is important to consider in order to understand the observed salt dependence of the kinetics. It is well known from melting experiments that DNA is more stable at high salt concentration due to a reduced repulsion between the strands of DNA in the presence of high concentration of counterions. This reduced repulsion in turn increases the flexibility of the DNA helix, making it more prone to bend (decreased electrostatic persistence length). An increased bending dynamics may also be associated with more frequent and larger base pair openings, which are required for dissociation of the thread-bound complexes. A kinetic investigation of the binding of the DNA analogue PNA to supercoiled DNA has thus suggested the base pair openings to be more frequent (for supercoiled DNA) at high salt concentration.[60] By contrast NMR experiments indicate that the rate of base pair openings in an oligomer is not dramatically dependent on the sodium concentration.[61]

Scheme 1

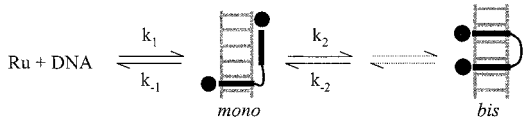

Our kinetics investigations show that the association reaction of **1** to DNA is complex: generally four exponentials are required to account for the experimental observed reaction rates. We propose that this complexity originates from a series of intermediate bound forms, as sketched in Figure 2. The association reaction is not only dependent on chirality of the binding compound but also on the choice of polynucleotide, as evident from Figure 7. As mentioned, earlier studies suggest that intercalation is a prerequisite for significant quantum yield of the bound complex. Our results then indicate that intercalation is faster with $[poly(dA\text{-}dT)]_2$ than with $[poly(dG\text{-}dC)]_2$. A similar behavior has also been observed for the threading intercalator nogalamycin and was then explained by the larger stability of G-C compared to A-T base pairs.[26] Despite the apparent complexity of the association reaction, we note that with a simple kinetics model (Scheme 1), using experimental data of the interaction of Δ-Δ **1** with $[poly(dA\text{-}dT)]_2$ it is possible to obtain a kinetic equilibrium constant that correlates well with that measured at steady-state. Still though, the kinetics upon association of Δ-Δ **1** to $[poly(dA\text{-}dT)]_2$ is far from completed on the time scale where the apparent rate constant used to form the $K_{kinetic}$ is measured. This observation indicates the need to include as well some slower reorganization processes (indicated by the dotted arrows in Scheme 1).

The depicted DNA complexes refer to mono- and bis-intercalated complexes, respectively. At the assumption that $k_1 \gg k_{-1}, k_2$, the measured second-ordered association rate constant (k_{a1}/[DNA] in eq 2) would be close to the true value of k_1 (Scheme 1). On the basis of the relatively large increase of the emission signal (preexponential factor) corresponding to k_{a1} (between 45 and 65% of the value after 500 s) we suggest that this step is the mono-intercalation of the complex. Furthermore, assuming that $k_{-1} \ll k_{-2} < k_2$ (k_{-1} thus corresponding to the rate-limiting step) the measured dissociation rate constant (k_d in eq 2) would be given by

$$k_d = k_{-1} \cdot \frac{1}{K'}$$

where

$$K' = \frac{[\text{bis}]}{[\text{mono}]} = \frac{k_2}{k_{-2}} \frac{k_3}{k_{-3}} \cdots\cdots \frac{k_n}{k_{-n}}$$

is the equilibrium constant between bis and mono intercalated forms, thus

$$\frac{k_1}{k_d} \approx K_{eq}$$

as evidenced from Figure 4. A further indication that the rate-

(60) Bentin, T.; Nielsen, P. E. *Biochemistry* **1996**, *35*, 8863−8869.
(61) Braunlin, W. H.; Bloomfield, V. A. *Biochemistry* **1988**, *27*, 1184−1191.

limiting step of dissociation here is from the mono-intercalated intermediate is the observation that the dissociation of the *meso* diastereomer (Δ-Λ) is almost as slow as that for the Δ-Δ enantiomer. Would bis → mono be rate-limiting, we would expect the Λ moiety to dissociate first, and *meso* to rather resemble Λ-Λ in dissociation kinetics.

The slow phase, observed most clearly as an increased amplitude of the LD spectrum, is most likely due to a reorganization of the complex providing regions on the DNA which have higher binding density (cooperative binding) and which, due to steric stiffness, will orient more efficiently in the flow and thus give a stronger LD signal. Since the increase in LD magnitude for the metal complex bands was not matched by a corresponding increase for the DNA nucleobase band, a local stiffening of DNA in the neighborhood of bound complexes was concluded. This mechanism necessarily involves an uneven distribution of bis-intercalated complexs in some stage: either an initial clustering of complexes that equilibrates into a more even distribution (kinetic cooperativity) or a more or less random initial distribution that clusters together upon equilibration (equilibrium cooperativity). At present we cannot readily tell which mechanism appears to be the more likely, however, for the latter mechanism a rather high cooperativity factor has to be involved to get significant different distributions of complexes over the persistence length of DNA (∼200 bp).

Conclusions

For the first time, dynamic selective DNA interaction properties have been directly observed for diastereomeric forms of a threading complex. The dimer in this study is particular because of its extremely high affinity for DNA as well as its remarkable bis-intercalative binding mode, which introduces topological constraints requiring the association and dissociation to occur via a threading mechanism. The threading makes the kinetics extremely slow and complex, requiring a multiexponential fitting function for the association reaction.

The dynamics is sensitive to the chirality of the dimer as opposed to the thermodynamic stability which shows merely small variation between the enantiomers: dissociation from ct-DNA is markedly faster and also more dependent on the ionic strength for the Λ-Λ compared to that for the Δ-Δ enantiomer.

Flow linear dichroism, finally, shows that there is also a very slow phase of the association reaction possibly associated with a redistribution of the bound dimers on the DNA lattice.

Acknowledgment. This study was defrayed by a grant to B.N. from the Swedish Natural Science Research Council (NFR).

Supporting Information Available: Amplitudes for biexponential fits of the dissociation of **1** with ct-DNA; experimental curves of association and dissociation of Δ-Δ **1** with [poly(dA-dT)]$_2$; dissociation kinetic data of Δ-Δ **1** with [poly(dG-dC)]$_2$ (PDF). This material is available free of charge via the Internet at http://pubs.acs.org.

JA003624D